Clin. Lab. 2027;73:XXX-XXX

ORIGINAL ARTICLE

Melatonin Effects on PI3K/Akt Pathway and Cognitive Function in Hypoxic Rat Hippocampal Neurons

Xinran Li [1, *], Xue Zhang [2, *], Conghui Liu [3], Jiabin Zhang [2], Qiancheng Chen [2], Xinhao Yuan [2], Xiaofei Song [4], Tiejun Liu [5], Yuedan Li [5], Yanlei Ge [2], Aishuang Fu [2]

[*] *These authors contributed equally to this work and should be considered co-first authors*
[1] *Clinical Medical College, North China University of Technology, Tangshan, Hebei, China*
[2] *Department of Respiratory Medicine, Affiliated Hospital of North China University of Technology, Tangshan, Hebei, China*
[3] *Department of Endocrinology, Affiliated Hospital of North China University of Technology, Tangshan, Hebei, China*
[4] *Department of Otorhinolaryngology, Hebei Provincial People's Hospital, Tangshan, Hebei, China*
[5] *Department of Anaesthesiology, Affiliated Hospital of North China University of Technology, Tangshan, Hebei, China*

ABSTRACT

Background: **This study aims to investigate whether melatonin improves cognitive dysfunction in rats, induced by intermittent hypoxia, by modulating the PI3K/Akt signaling pathway, using an intermittent hypoxia animal model.**

Methods: **Sixty-four male Wistar rats were randomly assigned to the following groups: normoxic control (UC), intermittent hypoxia (IH), PI3K inhibitor (PI3K-i), and melatonin intervention (MT), with n = 16 per group. Subgroups were distributed across 2-, 4-, 6-, and 8-week time points. Except for the UC group, all other groups underwent daily 7-hour IH exposure. The MT group and PI3K-i group received intraperitoneal injections of melatonin (10 mg/kg) or PI3K inhibitor GDC-0084 (20 mg/kg), respectively, prior to exposure. Cognitive function was assessed using the Morris water maze. Immunohistochemistry examined expression of p-PI3K, p-Akt, Nrf2, and HO-1 in the hippocampal CA1 region. Statistical analysis employed two-way ANOVA with Tukey's post hoc test; partial η^2 was reported.**

Results: **Behavioral data showed that the escape latency in the IH group significantly increased with prolonged exposure duration (2W: 21.30 ± 1.23 seconds, 8W: 55.61 ± 1.49 seconds), while the percentage of time spent in the target quadrant decreased (2W: 76.25 ± 1.72%, 8W: 22.76 ± 2.73%). The MT group demonstrated superior cognitive performance at all time points compared to the IH group (e.g., escape latency at 4 weeks: 28.74 ± 0.85 seconds vs. 32.24 ± 1.03 seconds, $p < 0.05$). Protein expression analysis revealed that p-PI3K, p-Akt, Nrf2, and HO-1 expression in both IH and MT groups exhibited an initial increase followed by a decrease, peaking at 4 weeks (e.g., IH group p-PI3K: 2.25 ± 0.09; MT group: 2.73 ± 0.05). Protein expression in the MT group was significantly higher than in the IH group (all $p < 0.05$), while expression in the PI3K-i group showed no significant difference from the UC group. Both treatment and time interactions were significant (e.g., p-PI3K: $F(9,48) = 189.18$, $p < 0.001$, $\eta^2 = 0.86$).**

Conclusions: **Melatonin may alleviate oxidative stress induced by intermittent hypoxia by regulating the PI3K/AKT signaling pathway and related antioxidant protein expression, thereby improving cognitive function in rats. PI3K inhibitors effectively blocked the upregulation of these proteins, whose expression levels showed no significant difference overall compared to the untreated group.**

(Clin. Lab. 2027;73:xx-xx. DOI: 10.7754/Clin.Lab.2026.260139)

Correspondence:
Yanlei Ge
North China University of Science and Technology Affiliated Hospital
Tangshan, Hebei
China
Phone: + 86 15932081296
Email: geyanlei@ncst.edu.cn

Aishuang Fu
North China University of Science and Technology Affiliated Hospital
Tangshan, Hebei
China
Phone: + 86 13393152699
Email: maxfas@163.com

Manuscript accepted February 9, 2026

KEYWORDS

intermittent hypoxia, oxidative stress, PI3K/Akt signaling pathway, melatonin, hippocampus

LIST OF ABBREVIATIONS

Akt - Protein kinase B
ANOVA - Analysis of variance
ARRIVE - Animal Research: Reporting of *In Vivo* Experiments guidelines
CA1 - Cornu ammonis area 1 (hippocampal subfield)
CI - Confidence interval
CIH - Chronic intermittent hypoxia
DAB - 3,3'-Diaminobenzidine
DMSO - Dimethyl sulfoxide
HO-1 - Heme oxygenase-1
IH - Intermittent hypoxia
IHC - Immunohistochemistry
MT - Melatonin-treated group
MWM - Morris water maze
Nrf2 - Nuclear factor erythroid 2-related factor 2
OSA/OSAS - Obstructive sleep apnea (syndrome)
PBS - Phosphate-buffered saline
PI3K - Phosphoinositide 3-kinase
p-Akt - Phosphorylated Akt
p-PI3K - Phosphorylated PI3K
QC - Quality control
SD - Standard deviation
UC - Normoxia/room-air control group

INTRODUCTION

Sleep apnea hypopnea syndrome (SAHS) refers to a clinical syndrome characterized by recurrent episodes of apnea, hypopnea, and hypercapnia during sleep, leading to multi-organ dysfunction [1]. It is characterized by recurrent episodes of intermittent hypoxia (IH) during sleep [2]. Given that brain tissue is most sensitive to ischemic and hypoxic injury, intermittent hypoxia causes the most pronounced damage to brain function, leading to cognitive impairment and significantly impacting quality of life [3,4]. Intermittent hypoxia plays a crucial role in the pathogenesis of cognitive dysfunction in SAHS patients. Therefore, identifying effective therapeutic interventions holds significant scientific value and societal importance.

Oxidative stress reflects an imbalance between oxidative processes and antioxidant defenses within the body. Within the antioxidant defense system, activation of the PI3K/Akt signaling pathway plays a pivotal role in exerting antioxidant effects and inhibiting apoptosis [5,6]. Repeated episodes of hypoxia-reoxygenation can induce oxidative stress, leading to central nervous system damage and cognitive dysfunction, and prompting the body to activate the PI3K/Akt signaling pathway.

Melatonin (N-acetyl-5-methoxytryptamine) is an indoleamine neuroendocrine hormone initially synthesized by the pineal gland in vertebrates. It exerts significant antioxidant activity and suppresses inflammatory responses within the body, playing a crucial role in neuroprotection [7-9]. Furthermore, under certain physiological or pathological conditions, melatonin can intervene in and scavenge endogenous oxygen free radicals, regulate pro-apoptotic and anti-apoptotic factors, upregulate anti-apoptotic proteins, and downregulate pro-apoptotic protein expression [10-12]. This study established an intermittent hypoxia model to investigate the protective effects of the antioxidant melatonin on intermittent hypoxia-induced neuronal apoptosis pathways. This provides a robust theoretical basis for applying melatonin intervention in SAHS-related cognitive impairment.

MATERIALS AND METHODS

Laboratory animals

Wistar adult male rats 64 (weight 170 ± 10 g), Animal License No. SCXK (Beijing) 2016-0002, purchased from Beijing Viton Lihua Laboratory Animal Science and Technology Co.

Main instrumentation and reagents

The water maze was purchased from Shanghai Yishu Information Technology Co., Ltd. (Dr. Rat), GDC-0084 (PI3K/Akt pathway inhibitor) was procured from Shanghai Lanmu Chemical Co., Ltd., p-PI3K antibody from Beijing Bio-Ocean Biotechnology Co., Ltd., p-Akt antibody, Nrf2 antibody, and HO-1 antibody from Cell Signaling Technology, Inc. (USA), DMSO from Sigma (USA), primary antibody diluent and secondary antibody diluent from Shanghai Yamei Biotechnology Co., Ltd., DAB coloring reagent purchased from Beijing Zhongshan Jinqiao Biotechnology Co., Ltd., PBS 0.01M powder purchased from Beijing Solarbio Technology Co., Ltd., phosphate buffer purchased from Beijing Zhongshan Jinqiao Biotechnology Co., Ltd., 0.01M sodium citrate buffer purchased from Beijing Solarbio Technology Co., Ltd., Anhydrous ethanol was purchased from Tianjin Continental Reagent Factory. Hematoxylin stain was purchased from Zhuhai Beisuo Biotechnology Co., Ltd. Eosin stain was purchased from Zhuhai Beisuo Biotechnology Co., Ltd. Neutral gum was purchased from Shanghai Yiyang Instruments Co., Ltd. Sodium hydroxide was purchased from Tianjin Oubokai Chemical Co., Ltd. Polyformaldehyde was purchased from Tianjin Oubokai Chemical Co., Ltd. Chloroform was purchased from Tianjin Oubokai Chemical Co., Ltd.

Animal grouping and intervention protocol

Using a random number table, 64 rats were randomly divided into four groups (n = 16 per group). Each group was then randomly and evenly distributed across four time points: 2, 4, 6, and 8 weeks (i.e., each treatment-

time subgroup had n = 4). (See Figure 1 for the animal grouping and intervention protocol flowchart.) Grouping and interventions were as follows: 1) Normal oxygen control group (UC group): Housed in an experimental chamber with continuous compressed air supply, maintaining chamber oxygen concentration at normal atmospheric levels (21% ± 0.5%). Exposure occurred daily from 08:00 to 15:00 for 2 - 8 consecutive weeks. 2) Intermittent Hypoxia Group (IH group): Placed in the experimental chamber daily from 08:00 to 15:00, receiving intermittent hypoxic exposure. The chamber oxygen concentration cycled between 5% and 21%, with each cycle lasting 120 seconds (comprising a 30-second reduction to 5% maintained for 30 seconds, followed by a 30-second restoration to 21% maintained for 30 seconds), for 7 hours daily. 3) PI3K inhibitor group (PI3K-i group): Thirty minutes prior to intermittent hypoxic exposure identical to the IH group (daily at 7:30), intraperitoneal injection of the PI3K/Akt pathway inhibitor GDC-0084. The drug was dissolved and diluted in physiological saline containing 5% DMSO and administered at a dose of 20 mg/kg. Injection volume was adjusted weekly according to body weight. 4) Melatonin group: Thirty minutes prior to the same intermittent hypoxic exposure as the IH group (daily at 7:30), intraperitoneal injection of melatonin solution (purchased from Sigma, catalogue number M5250), reconstituted in physiological saline, administered at a dose of 10 mg/kg. Injection volume adjusted weekly according to body weight.

Control group procedure: Rats in the UC and IH groups received intraperitoneal injections at the same daily time point (7:30) of an equal volume of physiological saline solvent containing 5% DMSO, identical to the PI3K-i group.

Preparation of Morris Water Maze specimens

Following the respective hypoxia/control exposures, water maze testing was conducted on the day before each time point (2, 4, 6, and 8 weeks). Each rat underwent six trials per day (three morning, three afternoon). Escape latency and time spent in the target quadrant were recorded, and the average values were used for analysis. The experimenter conducting and scoring the MWM tests was blinded to the group allocation of the rats.

Tissue sample collection and processing

Following completion of the water maze test, rats were deeply anesthetized via intraperitoneal injection of 20% urethane (0.5 mL/100 g). Following cardiac perfusion with physiological saline and 4% paraformaldehyde, the intact brain tissue was removed. On ice, hippocampal tissue was dissected; one portion was fixed in 4% paraformaldehyde for paraffin embedding and subsequent sectioning; another portion was rapidly placed in liquid nitrogen for freezing, then transferred to a -80°C freezer for storage and subsequent use.

Hippocampal tissue HE staining

Fixed hippocampal tissue underwent dehydration, clearing, and paraffin embedding prior to serial coronal sectioning (4 μm thickness). Sections were deparaffinized with xylene, hydrated with graded ethanol solutions, and subjected to hematoxylin-eosin staining. Following neutral resin mounting, the morphological structure of neurons in the hippocampal CA1 region was observed under an optical microscope and photographed.

Immunohistochemical detection

Paraffin sections (4 μm) were dewaxed and rehydrated, then placed in sodium citrate buffer (pH 6.0) for 20 minutes at 95℃ for antigen retrieval. Endogenous peroxidase was blocked with 3% H_2O_2 for 10 minutes, followed by blocking with 5% BSA for 30 minutes. Sections were incubated overnight at 4℃ with the following primary antibodies: p-PI3K (Beijing Bio-Ocean Biotechnology Co., Ltd., Cat. No. bs-5570R, 1:200), p-Akt (Cell Signaling Technology, Cat. No. 4060, 1:100), Nrf2 (Cell Signaling Technology, Cat. No. 12721, 1:200), HO-1 (Cell Signaling Technology, Cat. No. 43966, 1:200). The following day, biotinylated goat anti-rabbit IgG conjugate was added and incubated at room temperature for 30 minutes. DAB staining was performed, with nuclei counterstained using hematoxylin. PBS substituted for the primary antibody served as the negative control. The percentage of positive cells expressing the target protein in hippocampal tissue was observed and quantified under a microscope.

Quantification: Images were acquired using an Olympus optical microscope. For each section, three non-overlapping fields in the hippocampal CA1 region were selected. The percentage of positively stained cells and the mean optical density (MOD) were measured using Image-Pro Plus 6.0 software. The average value from three fields was used for statistical analysis. Inter-rater reliability was assessed on 20% of sections, with an intraclass correlation coefficient (ICC) of 0.91. Image quantification was performed by an investigator blinded to group assignments.

Statistical analysis

Statistical analysis was performed using SPSS 22.0 and JASP 0.18.3 software. Normality of distribution for quantitative data was confirmed by Shapiro-Wilk tests, and homogeneity of variance was demonstrated by Levene's tests. Data are presented as mean ± standard deviation ($\bar{x} \pm s$). Two-way ANOVA assessed the main effects of "treatment" and "time" and their interaction. Results included F-values, degrees of freedom, p-values, and partial effect size η^2 with 95% confidence intervals. If interaction was significant, simple effects analysis was performed, followed by Tukey HSD multiple comparison correction. Adjusted p values, mean differences (MD), and their 95% CIs were reported. For key intergroup comparisons, Cohen's d was additionally calculated as a standardized effect size. The significance level was set at $\alpha = 0.05$.

RESULTS

Morris Water Maze memory test results

Positioning navigation test

The results of the two-way ANOVA revealed significant main effects of "Treatment" ($F(3, 48) = 520.21$, $p < 0.001$, partial $\eta^2 = 0.96$, 95% CI [0.94, 0.97]) and a main effect of "Time" ($F(3, 48) = 387.92$, $p < 0.001$, partial $\eta^2 = 0.94$, 95% CI [0.92, 0.96]), and their interaction ($F(9, 48) = 464.44$, $p < 0.001$, partial $\eta^2 = 0.97$, 95% CI [0.95, 0.98]) were statistically significant. Simple effect analysis revealed statistically significant differences in escape latency among the four treatment groups at each intermittent hypoxic exposure time point (2W, 4W, 6W, 8W) ($p < 0.001$ at all time points). Subsequent Tukey-corrected pairwise comparisons at each time point revealed that the escape latency in the PI3K-i group was significantly longer than that in the IH group at all time points. The escape latency in the IH group was significantly longer than that in the MT group, and the escape latency in the MT group was significantly longer than that in the UC group (all comparisons adjusted $p < 0.05$). Effect size analysis at the 4W time point showed a Cohen's $d = 1.89$ (95% CI [1.12, 2.66]) for the escape latency difference between the MT and IH groups. As intermittent hypoxic exposure duration extended from 2 to 8 weeks, escape latency progressively increased in rats from the IH, MT, and PI3K-i groups (see Table 1).

Spatial exploration experiment

The results of the two-way ANOVA revealed significant main effects of “Treatment” ($F(3, 48) = 92.15$, $p < 0.001$, partial $\eta^2 = 0.85$, 95% CI [0.78, 0.90]) and “Time” ($F(3, 48) = 79.02$, $p < 0.001$, partial $\eta^2 = 0.83$, 95% CI [0.76, 0.88]), and their interaction ($F(9, 48) = 97.21$, $p < 0.001$, partial $\eta^2 = 0.90$, 95% CI [0.86, 0.93]) were statistically significant. Simple effects analysis revealed statistically significant differences in the percentage of time spent crossing the target quadrant among the four groups at all time points (2W, 4W, 6W, 8W) ($p < 0.001$ at each time point). Tukey-corrected pairwise comparisons at each time point revealed that the percentage in the PI3K inhibitor group was significantly lower than that in the IH group at all time points, while the IH group was significantly lower than the MT group, and the MT group was significantly lower than the UC group (all comparisons adjusted $p < 0.05$). At the 4W time point, the mean difference (MD) between the MT and IH groups was 6.25% (95% CI [4.88, 7.62]), with Cohen's $d = 1.52$ (95% CI [0.82, 2.22]). As intermittent hypoxic exposure duration increased, the percentage of time spent crossing the target quadrant gradually decreased in rats from the IH, MT, and PI3K inhibitor groups (see Table 2).

HE staining of rat hippocampal tissue

HE staining showed that the nerve cells in the normal group were well arranged and regular in morphology; with the prolongation of hypoxia, the nerve cells were gradually loosely arranged, the cytoplasm was sparse, and the edges of the cells were not clear under the microscope (see Figure 2).

Immunohistochemical expression changes of proteins related to the PI3K/Akt signaling pathway

Immunohistochemical results of p-PI3K protein in neurons of the hippocampal CA1 region across groups

Light microscopic observation of immunohistochemical staining revealed that p-PI3K protein expression was predominantly cytoplasmic in positive cells, appearing as brownish-yellow or light-yellow granules (see Figure 3).

Immunohistochemical results for p-PI3K protein in hippocampal CA1 neurons of rats

A two-way ANOVA revealed significant main effects of “Treatment” ($F(3, 48) = 134.09$, $p < 0.001$, partial $\eta^2 = 0.89$, 95% CI [0.85, 0.92]) and “Time” ($F(3, 48) = 155.77$, $p < 0.001$, partial $\eta^2 = 0.91$, 95% CI [0.87, 0.93]) and their interaction ($F(9, 48) = 189.18$, $p < 0.001$, partial $\eta^2 = 0.95$, 95% CI [0.93, 0.97]) were statistically significant. Simple effect analysis revealed significant differences in p-PI3K expression among the four groups at all time points (2W, 4W, 6W, 8W; all $p < 0.001$). Tukey-corrected pairwise comparisons within each time point revealed that MT group expression levels were significantly higher than IH group at all time points (e.g., 4W: MD = 0.48, 95% CI [0.41, 0.55], Cohen's $d = 2.67$), the IH group was significantly higher than the PI3K and UC groups, while no significant differences were observed between the PI3K-i and UC groups at any time point (adjusted $p > 0.05$). With prolonged intermittent hypoxia duration, p-PI3K expression in both the IH and MT groups exhibited an initial increase followed by a decrease, peaking at 4 weeks. In contrast, expression levels in the UC and PI3K-i groups remained stable at all time points (see Table 3).

Immunohistochemical results of p-Akt protein in rat hippocampal CA1 neuronal cells of each group

Immunohistochemical staining under the light microscope showed that the cytoplasm of the p-Akt protein positive cells was mainly colored with brownish yellow or light-yellow granules (see Figure 4).

A two-way ANOVA revealed significant main effects of “Treatment” ($F(3, 48) = 134.09$, $p < 0.001$, partial $\eta^2 = 0.89$, 95% CI [0.85, 0.92]) and “Time” ($F(3, 48) = 155.77$, $p < 0.001$, partial $\eta^2 = 0.91$, 95% CI [0.87, 0.93]), and interaction ($F(9, 48) = 189.18$, $p < 0.001$, partial $\eta^2 = 0.95$, 95% CI [0.93, 0.97]) were statistically significant. Simple effect analysis revealed significant between-group differences at all time points (all $p < 0.001$). Pairwise comparison trends aligned with p-PI3K: MT group > IH group > PI3K group ≈ UC group. At the 4-week time point, the difference in p-Akt expression between the MT group and the IH group was MD = 0.54 (95% CI [0.42, 0.66]), with Cohen's $d = 1.45$ (95% CI [0.76, 2.14]). p-Akt expression in the IH group peaked at week 4 and subsequently declined,

Table 1. Comparison of escape latency among groups of rats ($\bar{x} \pm s$, n = 4).

Groups	2W	4W	6W	8W
UC group	12.83 ± 2.24	12.73 ± 1.69	12.79 ± 2.58	13.27 ± 2.85
IH group	21.30 ± 1.23 [a]	32.24 ± 1.03 [a]	44.63 ± 2.04 [a]	55.61 ± 1.49 [a]
MT group	17.16 ± 0.81 [a, b]	28.74 ± 0.85 [a, b]	40.62 ± 1.41 [a, b]	52.65 ± 1.00 [a, b]
PI3K-i group	24.61 ± 1.35 [a, b, c]	36.14 ± 0.71 [a, b, c]	48.51 ± 1.31 [a, b, c]	59.20 ± 0.81 [a, b, c]

All groups in the table had n = 4 experimental animals at each observation time point. Pairwise comparison results (Tukey-corrected): Compared with the UC group, [a] $p < 0.05$; Compared with the IH group, [b] $p < 0.05$; Compared with the MT group, [c] $p < 0.05$.

Table 2. Comparison of percentage of time spent crossing the target among groups ($\bar{x} \pm s$, n = 4).

Groups	2W	4W	6W	8W
UC group	85.08 ± 2.28	85.33 ± 2.12	85.08 ± 2.04	85.13 ± 1.86
IH group	76.25 ± 1.72 [a]	57.42 ± 0.77 [a]	37.75 ± 2.13 [a]	22.76 ± 2.73 [a]
MT group	80.94 ± 2.11 [a, b]	63.67 ± 1.61 [a, b]	45.40 ± 0.81 [a, b]	27.41 ± 1.05 [a, b]
PI3K-i group	69.48 ± 1.24 [a, b, c]	52.89 ± 0.71 [a, b, c]	34.48 ± 1.88 [a, b, c]	15.47 ± 0.81 [a, b, c]

All groups in the table had n = 4 experimental animals at each observation time point. Pairwise comparison results (Tukey-corrected): Compared with the UC group, [a] $p < 0.05$; Compared with the IH group, [b] $p < 0.05$; Compared with the MT group, [c] $p < 0.01$.

Table 3. Expression of p-PI3K protein in neurons of the hippocampal CA1 region in rats from each group ($\bar{x} \pm s$, n = 4).

Groups	2W	4W	6W	8W
UC group	0.78 ± 0.09	0.80 ± 0.06	0.78 ± 0.06	0.75 ± 0.06
IH group	1.70 ± 0.09 [a]	2.25 ± 0.09 [a]	1.09 ± 0.05 [a]	1.02 ± 0.18 [a]
MT group	1.92 ± 0.03 [a, b]	2.73 ± 0.05 [a, b]	1.33 ± 0.02 [a, b]	1.16 ± 0.12 [a, b]
PI3K-i group	0.70 ± 0.13 [a, b, c]	0.78 ± 0.20 [a, b, c]	0.75 ± 0.02 [a, b, c]	0.75 ± 0.11 [a, b, c]

All groups in the table had n = 4 experimental animals at each observation time point. Pairwise comparison results (Tukey-corrected): Compared with the UC group, [a] $p < 0.05$; Compared with the IH group, [b] $p < 0.05$; Compared with the MT group, [c] $p < 0.05$.

Table 4. p-Akt protein expression in immunohistochemical neurons of the hippocampal CA1 region in each group of rats ($\bar{x} \pm s$, n = 4).

Groups	2W	4W	6W	8W
UC group	0.97 ± 0.05	0.97 ± 0.06	0.99 ± 0.05	0.99 ± 0.06
IH group	1.52 ± 0.13 [a]	2.14 ± 0.04 [a]	1.67 ± 0.05 [a]	1.21 ± 0.04 [a]
MT group	1.83 ± 0.04 [a, b]	2.68 ± 0.22 [a, b]	1.75 ± 0.07 [a, b]	1.39 ± 0.03 [a, b]
PI3K-i group	1.10 ± 0.11 [a, b, c]	1.16 ± 0.05 [a, b, c]	1.13 ± 0.03 [a, b, c]	1.11 ± 0.09 [a, b, c]

All groups in the table had n = 4 experimental animals at each observation time point. Pairwise comparison results (Tukey-corrected): Compared with the UC group, [a] $p < 0.05$; Compared with the IH group, [b] $p < 0.05$; Compared with the MT group, [c] $p < 0.05$.

Table 5. Immunohistochemical expression of Nrf2 protein in hippocampal CA1 neurons of rats across groups ($\bar{x} \pm s$, n = 4).

Groups	2W	4W	6W	8W
UC group	0.94 ± 0.11	0.94 ± 0.07	0.94 ± 0.12	0.98 ± 0.10
IH group	2.65 ± 0.06 [a]	3.32 ± 0.07 [a]	2.15 ± 0.03 [a]	1.65 ± 0.06 [a]
MT group	2.79 ± 0.07 [a, b]	3.65 ± 0.08 [a, b]	2.27 ± 0.05 [a, b]	1.86 ± 0.03 [a, b]
PI3K-i group	2.49 ± 0.05 [a, b, c]	3.11 ± 0.09 [a, b, c]	1.97 ± 0.06 [a, b, c]	1.35 ± 0.06 [a, b, c]

All groups in the table had n = 4 experimental animals at each observation time point. Pairwise comparison results (Tukey-corrected): Compared with the UC group, [a] $p < 0.05$; Compared with the IH group, [b] $p < 0.05$; Compared with the MT group, [c] $p < 0.05$.

Table 6. Expression of HO-1 protein in immunohistochemical neurons of the hippocampal CA1 region in rats from each group ($\bar{x} \pm s$, n = 4).

Groups	2W	4W	6W	8W
UC group	1.02 ± 0.13	1.03 ± 0.13	1.02 ± 0.11	1.04 ± 0.11
IH group	3.46 ± 0.04 [a]	4.11 ± 0.05 [a]	2.75 ± 0.06 [a]	1.78 ± 0.15 [a]
MT group	3.65 ± 0.05 [a, b]	4.28 ± 0.07 [a, b]	3.07 ± 0.02 [a, b]	2.54 ± 0.10 [a, b]
PI3K-i group	3.18 ± 0.06 [a, b, c]	3.92 ± 0.13 [a, b, c]	2.89 ± 0.03 [a, b, c]	1.47 ± 0.07 [a, b, c]

All groups in the table had n = 4 experimental animals at each observation time point. Pairwise comparison results (Tukey-corrected): Compared with the UC group, [a] $p < 0.05$; Compared with the IH group, [b] $p < 0.05$; Compared with the MT group, [c] $p < 0.05$.

whereas no significant temporal fluctuations were observed in the UC or PI3K-i groups (see Table 4).

Immunohistochemical results of Nrf2 protein in rat hippocampal CA1 neuronal cells in each group

Immunohistochemical staining under the light microscope showed that Nrf2 protein-positive cells were mainly cytoplasmic, with brownish-yellow or light-yellow granules (see Figure 5).

The results of the two-way ANOVA revealed significant main effects of "Treatment" ($F(3, 48) = 299.37$, $p < 0.001$, partial $\eta^2 = 0.95$, 95% CI [0.93, 0.97]) and "Time" ($F(3, 48) = 92.40$, $p < 0.001$, partial $\eta^2 = 0.85$, 95% CI [0.79, 0.89]), and interaction ($F(9, 48) = 107.81$, $p < 0.001$, partial $\eta^2 = 0.91$, 95% CI [0.88, 0.94]) were statistically significant. Simple effect analysis confirmed significant between-group differences at all time points (all $p < 0.001$). Tukey-corrected pairwise comparisons within each time point revealed: MT group > IH group > PI3K-i group > UC group (all adjusted $p < 0.05$). At the peak time point (4W), the difference in Nrf2 expression between the MT and IH groups was MD = 0.33 (95% CI [0.28, 0.38]), Cohen's $d = 1.65$ (95% CI [0.94, 2.36]). Nrf2 expression in the IH, MT, and PI3K-i groups showed an initial increase followed by a decrease, peaking at 4 weeks. Expression in the UC group showed no temporal variation (see Table 5).

Immunohistochemical results of HO-1 protein in rat hippocampal CA1 neuronal cells of various groups

Immunohistochemical staining under the light microscope showed that the cytoplasm of HO-1 protein-positive cells was mainly colored with brown-yellow or light-yellow granules (see Figure 6).

Immunohistochemical results of HO-1 protein in rat hippocampal CA1 region nerve cells

Two-way ANOVA revealed significant main effects of "Treatment" ($F(3, 48) = 140.94$, $p < 0.001$, partial $\eta^2 = 0.90$, 95% CI [0.86, 0.93]) and "Time" ($F(3, 48) = 90.99$, $p < 0.001$, partial $\eta^2 = 0.85$, 95% CI [0.79, 0.89]), and interaction ($F(9, 48) = 115.80$, $p < 0.001$, partial $\eta^2 = 0.90$, 95% CI [0.86, 0.93]). Simple effect analysis revealed significant intergroup differences at all time points (all $p < 0.001$). Tukey-corrected pairwise comparisons showed a trend consistent with Nrf2: MT group > IH group > PI3K-i group > UC group (all comparisons adjusted $p < 0.05$). At the 4W time point, the difference in HO-1 expression between the MT and IH groups was MD = 0.17 (95% CI [0.12, 0.22]), Cohen's $d = 0.95$ (95% CI [0.31, 1.59]). HO-1 expression levels peaked at 4 weeks in the IH, MT, and PI3K-i groups before declining; expression remained stable in the UC group (see Table 6).

The results above indicate that intermittent hypoxia dynamically regulates the expression of key proteins in the PI3K/Akt signaling pathway (p-PI3K, p-Akt) and their downstream antioxidant proteins (Nrf2, HO-1) in the hippocampal CA1 region, with expression peaking at 4 weeks of exposure. Melatonin intervention further enhances the expression of these proteins, while the PI3K/Akt pathway inhibitor GDC-0084 effectively blocks the upregulation of these proteins induced by intermittent

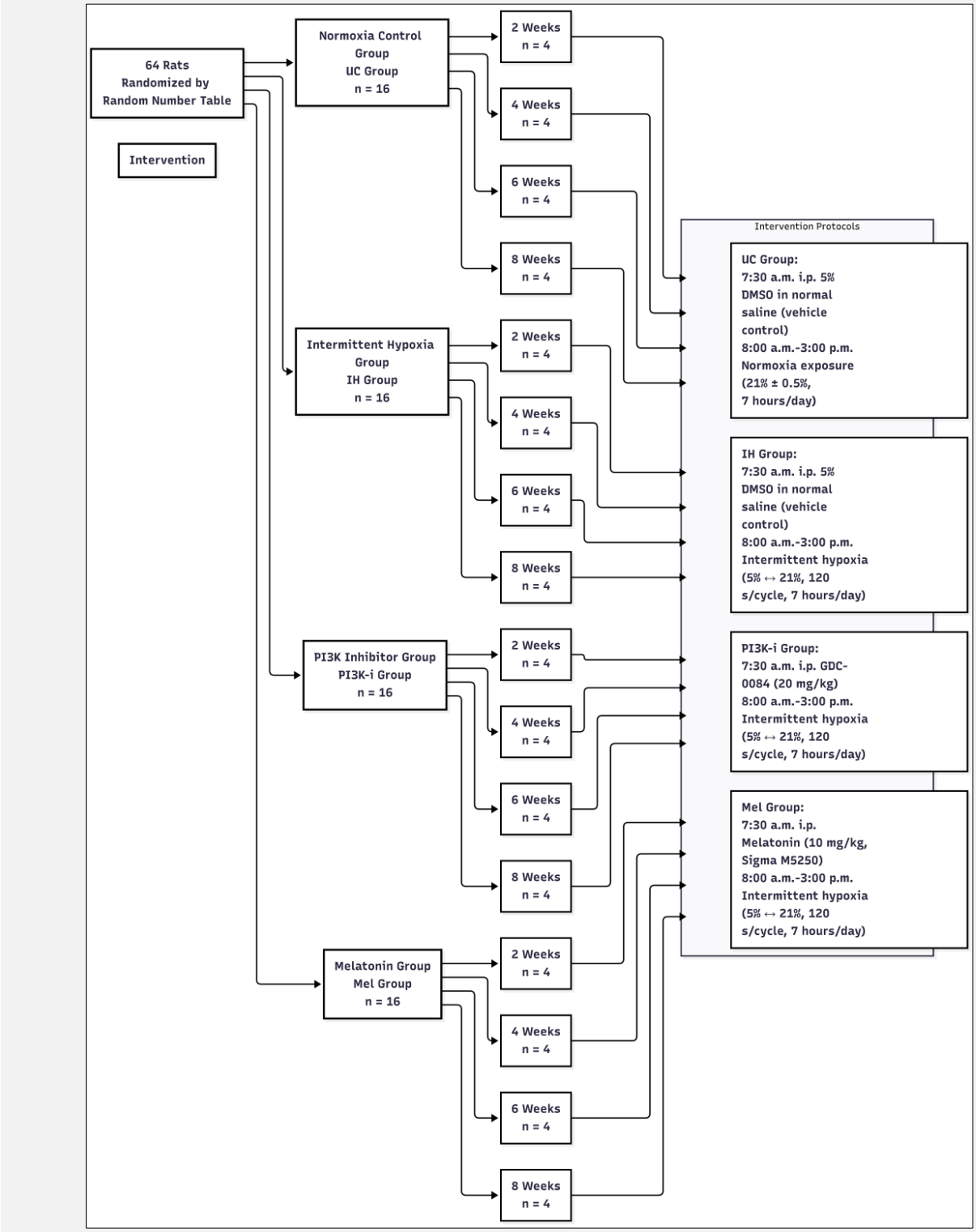

Figure 1. Flow chart of animal grouping and intervention protocols.

A total of 64 rats were randomly allocated into four groups (n = 16 per group) via a random number table method. Each group was further equally divided into four time points (2, 4, 6, and 8 weeks, n = 4 per subgroup). Corresponding interventions were administered daily for the designated duration. UC: normoxia control, IH: intermittent hypoxia, PI3K-i: PI3K inhibitor, Mel: melatonin, i.p.: intraperitoneal injection, h/d: hours per day.

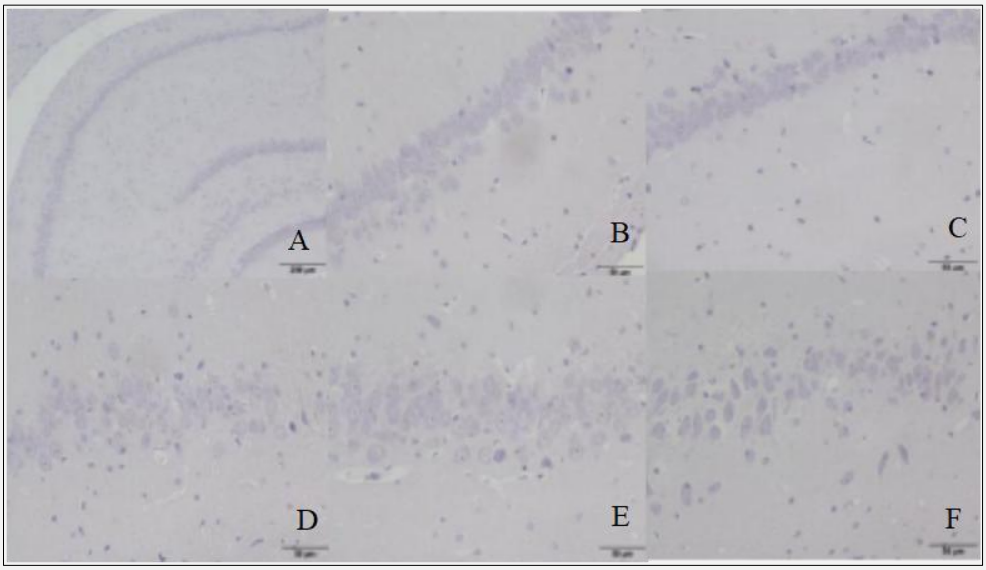

Figure 2. Hematoxylin and eosin (HE) staining of the hippocampal CA1 region in intermittent hypoxia-exposed rats (4 μm).

A, B: Control group, C: IH 2W group, D: IH 4W group, E: IH 6W group, F: IH 8W group.

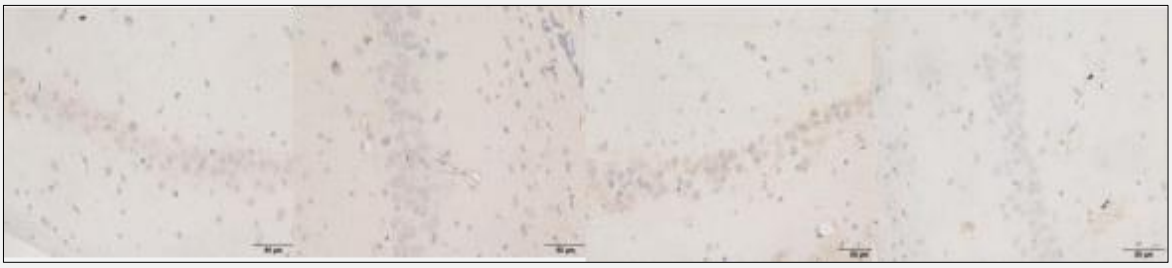

Figure 3. Expression of p-PI3K protein in hippocampal CA1 neurons of rats in each group (immunohistochemistry, 4 μm).

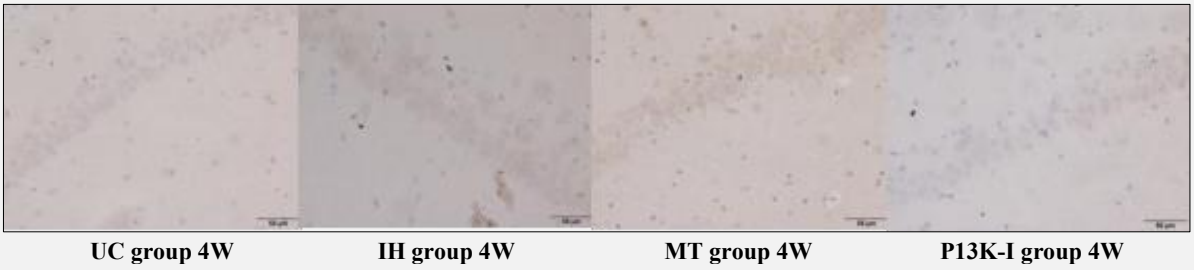

Figure 4. Expression of p-Akt protein in hippocampal CA1 neurons of rats across groups (immunohistochemistry, 4 μm).

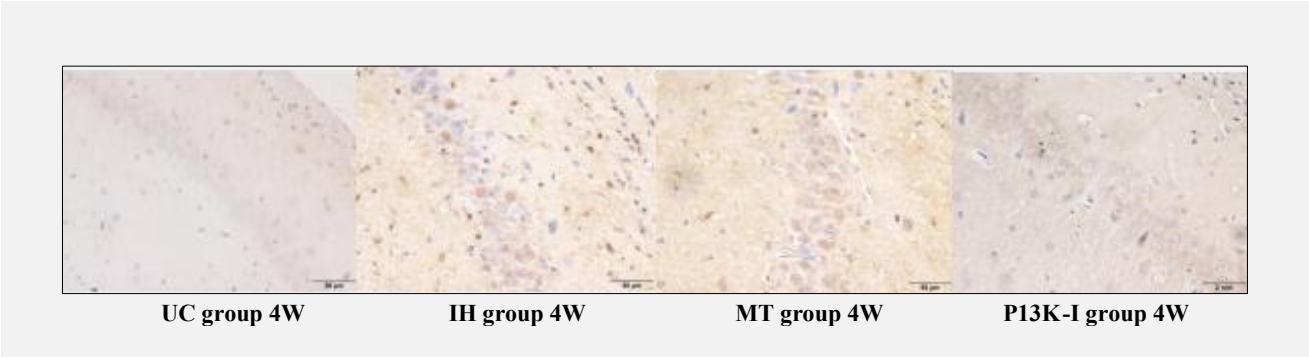

Figure 5. Expression of Nrf2 protein in hippocampal CA1 neurons of rats in each group (immunohistochemistry, 4 μm).

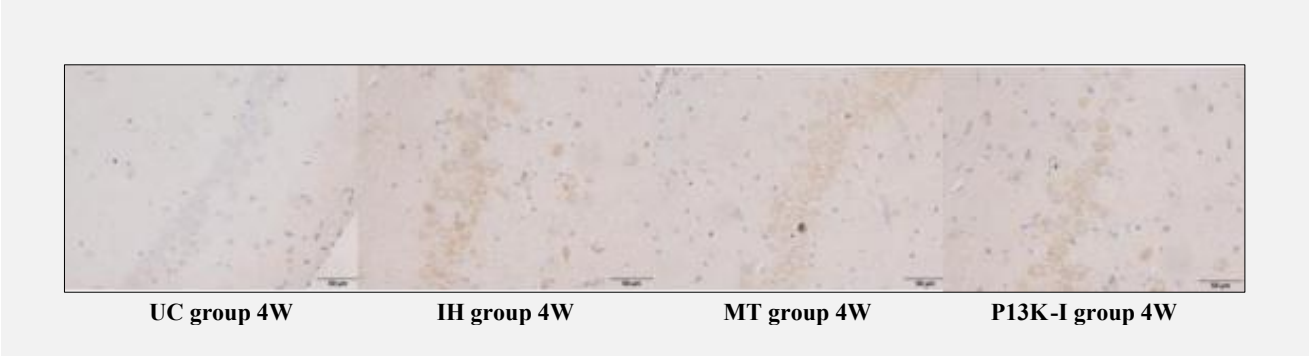

Figure 6. Expression of HO-1 protein in hippocampal CA1 neurons of rats in each group (immunohistochemistry, 4 μm).

hypoxia and melatonin.

DISCUSSION

Sleep-disordered breathing-associated cognitive impairment is a significant complication affecting patients' quality of life. The core pathophysiological mechanism by which chronic intermittent hypoxia (IH) leads to hippocampal damage remains to be fully elucidated [13, 14]. This study established an IH rat model and demonstrated that melatonin alleviates IH-induced progressive impairment in spatial learning and memory by activating the PI3K/Akt/Nrf2 signaling axis. Key findings include: 1) IH caused progressive cognitive decline in rats, accompanied by a dynamic pattern in the hippocampal CA1 region: initial induction (peaking at 4 weeks) followed by depletion of PI3K/Akt pathway and downstream Nrf2/HO-1 antioxidant protein expression; 2) Melatonin intervention significantly improved behavioral deficits while enhancing and sustaining expression of these pathway proteins; 3) Treatment with the PI3K/Akt inhibitor GDC-0084 completely blocked melatonin's protective effects and exacerbated injury, providing reverse validation of this pathway's critical mediating role.

Progressive cognitive impairment induced by intermittent hypoxia and the mitigating effects of melatonin

Research on intermittent hypoxia-induced cognitive impairment has garnered significant attention, with studies demonstrating that intermittent hypoxia can disrupt neuronal cells and neural signaling pathways, leading to cognitive decline [15,16]. The hippocampus plays a crucial role in long-term memory formation. This study employed the Morris water maze, a classic paradigm for assessing hippocampus-dependent spatial memory. Results clearly demonstrated that rats exhibited prolonged escape latency and reduced target quadrant exploration time starting from 2 weeks of IH exposure, with impairment severity increasing with prolonged exposure duration. This precisely mimics the cumulative cognitive damage observed in the clinical course of SAHS and suggests that hippocampal neurons become vulnerable targets early in IH exposure. Notably, melatonin treatment consistently mitigated this impairment throughout the 8-week observation period, with significantly supe-

rior behavioral performance compared to the IH group at all time points. These findings provide direct preclinical evidence that melatonin ameliorates SAHS-related cognitive dysfunction.

Dynamic response and exhaustion of the PI3K/Akt/Nrf2 signaling axis under intermittent hypoxia stress

The body has developed a complex antioxidant defense system against oxidative stress, encompassing mechanisms such as defense, protection against oxidative damage, clearance of oxygen free radicals, elimination of H_2O_2, removal of superoxide anion radicals, maintenance of cellular redox balance, and prevention of oxidative injury. Numerous studies have demonstrated that the PI3K/Akt signaling pathway plays a crucial protective role in cerebral hypoxic-ischemic injury [17]. We further explored the molecular mechanisms underlying behavioral phenotypes. This study revealed that the expression of phosphorylated PI3K, Akt, and their downstream transcription factor Nrf2, as well as the antioxidant enzyme HO-1, in the hippocampal CA1 region exhibited a consistent "initial increase followed by decrease" trend in both IH and MT groups, peaking at 4 weeks. This dynamic pattern carries profound pathophysiological implications: during early IH stress, cells may activate endogenous protective programs by engaging the PI3K/Akt pathway. Activated Akt promotes nuclear translocation of Nrf2, which in turn upregulates phase II antioxidant enzymes like HO-1, collectively forming a defense system against oxidative stress. However, as IH persists (6 - 8 weeks), this compensatory activation may fail to counteract sustained oxidative damage, leading to pathway exhaustion and collapse of antioxidant defenses - a timeline consistent with progressive cognitive decline. Our findings provide protein-level evidence supporting the hypothesis that "IH ultimately exhausts antioxidant compensatory mechanisms".

Core mechanism of melatonin's neuroprotective action: activation and maintenance of PI3K/Akt/Nrf2 pathway activity

Melatonin is renowned for its potent free radical scavenging capacity and indirect antioxidant properties [18-20]. One of the most significant findings of this study is the identification of the PI3K/Akt pathway as the central hub for melatonin's neuroprotective effects. Compared to the IH group, melatonin intervention further elevated peak expression levels of p-PI3K, p-Akt, Nrf2, and HO-1, while also delaying their subsequent decline. More critically, the specific inhibitor GDC-0084 not only completely blocked melatonin's cognitive-enhancing effects but also worsened behavioral and molecular indicators to levels below those of the IH-only group. This gain-of-function/loss-of-function experimental design powerfully demonstrates that melatonin's benefits are largely dependent on its activation of the PI3K/Akt pathway.

Melatonin integrates multi-level protective effects through this pathway: 1) At the antioxidant level, it enhances Nrf2 stability and transcriptional activity via Akt, systematically upregulating endogenous antioxidant defense networks such as HO-1 [19]; 2) At the anti-apoptotic level, Akt phosphorylates and inhibits pro-apoptotic factors like Bad and Caspase-9, promoting neuronal survival [21,22]. The protective effect of melatonin on hippocampal neuronal morphology observed in this study results from its synergistic anti-oxidative stress and anti-apoptotic actions. Furthermore, recent research suggests that the antioxidant network formed by melatonin and its metabolites may contribute to its long-lasting effects [23], providing new directions for future studies.

Research limitations and future directions

This study has several limitations. First, the intermittent hypoxia model primarily mimics chronic hypoxia and does not fully capture other clinical features of sleep apnea syndrome (such as sleep fragmentation). Second, the study did not directly validate molecular regulatory relationships upstream or downstream of the pathway nor explore other critical mechanisms like neuroinflammation. Third, the sample size per time point was relatively small (n = 4), which may limit statistical power. Additionally, while outcome assessment was blinded, the administration of interventions could not be fully blinded. The study was conducted only in male rats, limiting generalizability to females. Finally, the controlled chamber model may not fully replicate the complexity of human OSA.

Therefore, future research should develop more integrated animal models and employ techniques like genetic manipulation to directly validate pathway mechanisms at the molecular level. Concurrently, multi-omics approaches should be used to systematically reveal melatonin's functional networks.

Expanding sample sizes and conducting multidimensional behavioral assessments will ultimately facilitate clinical translation through dose optimization and combination therapy studies.

CONCLUSION

In summary, this study reveals a key mechanism by which chronic intermittent hypoxia impairs cognitive function: the dynamic imbalance and depletion of the endogenous protective axis PI3K/Akt/Nrf2. Furthermore, we demonstrated in the SAHS model that melatonin effectively mitigates hippocampal injury and cognitive decline by targeting, activating, and sustaining this pathway. This provides crucial theoretical and experimental foundations for developing melatonin or its derivatives targeting the PI3K/Akt/Nrf2 axis as adjunctive therapeutic strategies for SAHS-related cognitive impairment.

Acknowledgment:
We gratefully acknowledge the valuable suggestions provided by colleagues at the Affiliated Hospital of North China University of Science and Technology and Hebei Provincial People's Hospital.

Source of Support:
This study was supported by the 2025 Hebei Province Medical Application Technology Tracking Project [GZ 20250080] and the Hebei Provincial Department of Education Grant Program for Fostering Innovation Skills Among Current Graduate Students [CXZZSS2025056].

Ethical Approval:
This study was approved by the Animal Ethics Committee of North China University of Science and Technology (Approval No. LX2019069). All procedures were performed in accordance with the ARRIVE guidelines and institutional animal care standards.

Declaration of Generative AI in Scientific Writing:
In the preparation of this manuscript, generative AI tools, including ChatGPT and DeepSeek, were used to assist with language polishing and manuscript title refinement. All content, including the revised title and scientific narrative, was reviewed, edited, and approved by the authors to ensure accuracy, scientific rigor, and compliance with ethical standards. The authors retain full responsibility for the originality, validity, and integrity of all research content. No AI-generated content was presented as original research data or findings.

Declaration of Interest:
The authors declare no competing interests.

References:

1. Berger S, Polotsky VY. Leptin and Leptin Resistance in the Pathogenesis of Obstructive Sleep Apnea: A Possible Link to Oxidative Stress and Cardiovascular Complications. Oxid Med Cell Longev 2018 Feb 20;2018:5137947. (PMID: 29675134)

2. Prabhakar NR, Peng YJ, Nanduri J. Hypoxia-inducible factors and obstructive sleep apnea. J Clin Invest 2020 Oct 1;130(10):5042-51. (PMID: 32730232)

3. Sehr T, Akgün K, Benkert P, Kuhle J, Ziemssen T, Brandt MD. Effects of obstructive sleep apnea treatment on neurodegenerative biomarker neurofilament light chain and cognitive performance. J Sleep Res 2024 Oct;33(5):e14164. (PMID: 38351662)

4. McNicholas N, Russell A, Nolan G, et al. Impact of obstructive sleep apnoea on cognitive function in multiple sclerosis: A longitudinal study. J Sleep Res 2021 Jun;30(3):e13159. (PMID: 32791570)

5. Zhang H, Huang H, Miao F, Nan J. Sea buckthorn flavonoids attenuate oxidative stress in hepatocellular carcinoma via suppression of PI3K/Akt and JAK pathways. Am J Transl Res 2025 Dec 15;17(12):9830-45. (PMID: 41552304)

6. Ismail A, Abdou FY, Gharib OA, et al. Potent Antioxidant and Anti-Inflammatory Metabolites of Pongamia pinnata Stems and Their Role in NF-κB and PI3K/Akt/mTOR Signaling Pathways Regulation in Irradiated Rats. Chem Biodivers 2026 Jan;23(1):e02776. (PMID: 41532875)

7. Giri A, Mehan S, Khan Z, Das Gupta G, Narula AS, Kalfin R. Modulation of neural circuits by melatonin in neurodegenerative and neuropsychiatric disorders. Naunyn Schmiedebergs Arch Pharmacol 2024 Jun;397(6):3867-95. (PMID: 38225412)

8. Hardeland R. Melatonin and inflammation-Story of a double-edged blade. J Pineal Res 2018 Nov;65(4):e12525. (PMID: 30242884)

9. Salman M, Kaushik P, Tabassum H, Parvez S. Melatonin Provides Neuroprotection Following Traumatic Brain Injury-Promoted Mitochondrial Perturbation in Wistar Rat. Cell Mol Neurobiol 2021 May;41(4):765-81. (PMID: 32468441)

10. Zuo J, Jiang Z. Melatonin attenuates hypertension and oxidative stress in a rat model of L-NAME-induced gestational hypertension. Vasc Med 2020 Aug;25(4):295-301. (PMID: 32469270)

11. D'Angelo G, Chimenz R, Reiter RJ, Gitto E. Use of Melatonin in Oxidative Stress Related Neonatal Diseases. Antioxidants (Basel) 2020 Jun 2;9(6):477. (PMID: 32498356)

12. Ferreira de Melo IM, Martins Ferreira CG, Lima da Silva Souza EH, et al. Melatonin regulates the expression of inflammatory cytokines, VEGF and apoptosis in diabetic retinopathy in rats. Chem Biol Interact 2020 Aug 25;327:109183. (PMID: 32554039)

13. Lavie L. Oxidative stress in obstructive sleep apnea and intermittent hypoxia-revisited-the bad ugly and good: implications to the heart and brain. Sleep Med Rev 2015 Apr;20:27-45. (PMID: 25155182)

14. Ryan S, Cummins EP, Farre R, et al. Understanding the pathophysiological mechanisms of cardiometabolic complications in obstructive sleep apnoea: towards personalised treatment approaches. Eur Respir J 2020 Aug 6;56(2):1902295. (PMID: 32265303)

15. Qi KR, Chen X, Si JC, Yang SC. [Research progress on chronic intermittent hypoxia and cognitive impairment]. Sheng Li Xue Bao 2024 Oct 25;76(5):752-60. (PMID: 39468811)

16. Li L, Ren F, Qi C, et al. Intermittent hypoxia promotes melanoma lung metastasis via oxidative stress and inflammation responses in a mouse model of obstructive sleep apnea. Respir Res 2018 Feb 12;19(1):28. (PMID: 29433520)

17. Zheng B, Qi J, Yang Y, et al. Mechanisms of cinnamic aldehyde against myocardial ischemia/hypoxia injury *in vivo* and *in vitro*: Involvement of regulating PI3K/Akt signaling pathway. Biomed Pharmacother 2022 Mar;147:112674. (PMID: 35093758)

18. Samanta S. Physiological and pharmacological perspectives of melatonin. Arch Physiol Biochem 2022 Oct;128(5):1346-67. (PMID: 32520581)

19. Sethi P, Mehan S, Khan Z, et al. The SIRT-1/Nrf2/HO-1 axis: Guardians of neuronal health in neurological disorders. Behav Brain Res 2025 Jan 5;476:115280. (PMID: 39368713)

20. Reiter RJ, Sharma RN, Manucha W, et al. Dysfunctional mitochondria in age-related neurodegeneration: Utility of melatonin as an antioxidant treatment. Ageing Res Rev 2024 Nov;101:102480. (PMID: 39236857)

21. Koh PO. Melatonin prevents hepatic injury-induced decrease in Akt downstream targets phosphorylations. J Pineal Res 2011 Sep;51(2):214-9. (PMID: 21492218)

22. Kim CH, Kim KH, Yoo YM. Melatonin protects against apoptotic and autophagic cell death in C2C12 murine myoblast cells. J Pineal Res 2011 Apr;50(3):241-9. (PMID: 21138475)

23. Xu G, Dong Y, Wang Z, et al. Melatonin Attenuates Oxidative Stress-Induced Apoptosis of Bovine Ovarian Granulosa Cells by Promoting Mitophagy via SIRT1/FoxO1 Signaling Pathway. Int J Mol Sci 2023 Aug 16;24(16):12854. (PMID: 37629033)